Interpretable Surrogate Modeling of Peak Heat Exchange Capacity in Thermally Activated Planar Retaining Walls

Dr. Rafay Tallat[1,*] and Dr. Naresh Chandra[1]

[1] Indian Institute of Technology Delhi Hauz Khas,New Delhi-110016
* Correspondence: rafya.tal@iitd.ac.in

Abstract: Thermally active retaining walls can be designed both as support for excavation and as shallow geothermal systems, but their thermal behaviour cannot be readily evaluated at the preliminary design stage because it relies on simultaneous interaction between the shape of the wall, its thermal conductivity and the temperature difference between the ground side and the excavated side. In this work we develop a surrogate model for peak heating season heat exchange of planar retaining walls using a numerically generated database which contains three kinds of cases: the short-duration heat-exchange cases, the geometry-response cases with deep walls and the conductivity-response cases. The purpose of the modelling is not to substitute computationally intensive simulation but to generate a transparent design relationship which would highlight and quantify the major factors involved. The analysis demonstrates that short-duration heat exchange estimates are primarily controlled by the near-wall thermal condition and wall thermal conductivity whereas moderate variations in the external boundary conditions yield relatively minor perturbations. Among all the geometric parameters which describe retaining wall in the seasonal design space the main factor is the composite value of $(H/L)/D$. The Results and Discussion sections continue the analysis of the fitted response using sensitivity derivatives, elasticities, threshold thickness analysis, material compensation analysis and uncertainty propagation. Conductivity analysis indicates that within the explored range the thermal resistance of the wall plays much more important role than the thermal resistance of the soil. A regressional model which is based on the excavation ratio, wall thickness, wall depth, soil conductivity and wall conductivity replicates the assembled design database with high accuracy ($R^2 = 0.997$) and preserves good prediction power in the leave-one-geometry-out cross-validation mode ($R^2 = 0.985$). It can thus be concluded that the equation derived is useful for evaluating the viability of deep retaining walls through thermal analysis at an early stage.

Citation: Dr. Rafay Tallat and Dr. Naresh Chandra. 2025. Interpretable Surrogate Modeling of Peak Heat Exchange Capacity in Thermally Activated Planar Retaining Walls. *TK Techforum Journal (ThyssenKrupp Techforum)* 2024(3): 28–41.

Received: July-08-2024
Accepted: December 15-2024
Published: January-30-2025

Keywords: energy walls; energy geostructures; retaining walls; shallow geothermal systems; surrogate modeling; response surface; thermal design

1. Introduction

Reduction in the carbon intensity of buildings and underground construction is increasingly calling for heating and cooling systems that exploit the earth as a steady thermal reservoir without a demand for expansive surface area. Shallow geothermal systems are able to meet this demand in many cases, but the availability of land and its possible congestion, the presence of underground utilities, and the high costs of geothermal drilling impose certain limitations on borehole fields. Thus, interest in energy geostructures, in which the heat exchanger functions are carried out by components of the construction that are necessary for load transfer or earth retention anyway, has become more widespread [1,2]. Energy geostructures may be especially beneficial in dense urban environment where structural surfaces are abundant while land availability is limited [3].

A special class of energy geostructure is formed by thermally activated retaining walls. These are employed in the construction of basements, underground stations, cut-and-cover corridors, parking structures, and deep urban excavations, where extensive

wall sections are frequently available. Experiments and numerical modelling showed that diaphragm and embedded retaining walls can be efficient heat exchangers if pipe circuits are embedded in their concrete mass [4,5]. Nevertheless, the behavior of such walls is fundamentally different from borehole heat exchangers and energy piles as a retaining wall is simultaneously exposed to two very different thermal conditions: one of them corresponds to the interaction with the ground mass, and the other may correspond to the interface with an excavation, an underground room, or a boundary of the system that is controlled by the building operation [6].

Such an asymmetry of thermal exposures is the source of a complex design task in which the geometrical properties of the retaining wall, material conductivities, and boundary conditions cannot be separated [7]. The thickness of the wall defines the conductive pathway between the embedded pipes and the excavated face, the depth of the excavation is responsible for the share of wall face that is thermally exposed, the depth of the whole wall determines the role of the upper boundary, and the conductivities of soil and concrete determine the resistance of the pathway for heat transfer. It was demonstrated previously that these variables affect the performance of energy walls and retaining wall heat exchangers in a crucial way [8,9]. Other parametric studies revealed that the arrangement of pipes, ground properties, and operating schedule could affect the magnitude and timing of heat transfer [10–12].

The full-scale thermo-hydro-mechanical numerical modeling is always necessary in the final stage of project design, especially if groundwater flow, the mechanical effect of the retaining wall, staged excavation or coupled operation with the building are essential [13]. However, a different kind of tool is needed at the early stage of a project. At the beginning of the project, the engineers may require a clear relation that would allow determining whether a particular retaining wall design is thermally promising, what variables define its response, and whether material or geometric modifications will lead to useful changes [14]. A low-order surrogate model could help with providing this information, if its variables and coefficients retain physical interpretability [15].

The response-surface and surrogate modeling techniques have been widely used in engineering design for constructing an explicit equation from a limited number of simulations [16]. Their usefulness in the current context goes beyond the purely computational speed. An explicit equation would reveal the mechanism of the combined effect of the ratio of the excavation and wall thickness on the heat exchange. The importance of such a relation is based on the fact that it should respect the thermal structure of the problem. In energy retaining walls, the most important interaction is expected to be between the share of the thermal exposure of the wall and its thickness because the effectiveness of this exposure should decrease with increasing thickness of the wall [17,18].

The research question in this paper is therefore clearly stated: can the peak heat exchange of a thermally activated planar retaining wall in the heating season be represented by a low-order surrogate that would identify the main geometric and conductivity effects without losing physical interpretability? To answer this question, the study uses a case set for numerical modeling, which is split into the set of short-term diagnostic cases, the set of geometry-response cases for the entire season and the set of conductivity variations. The analysis will rank the most important short-term perturbations, find the main geometry descriptor for seasonal response, compare the effect of the soil and wall conductivities and construct an explicitly formulated relation for preliminary design.

2. Numerical case basis and modeling process

2.1. Subsets of cases

In this work, the numerical modeling employs three different kinds of numerical cases. The first kind includes 48 hours cases, where the initial temperature, boundary temperature, and wall thermal conductivity are varied in order to find out the most significant factors for a short period. The second kind includes seasonal response peak cases, in which deep planar retaining walls with some specified ratios of excavation, wall depth, and

wall thickness are used. The third kind includes conductivity varying cases with typical geometry and provides the first-order material effect in the final equation.

Table 1 is essential in order not to make three types of case groups to fulfill the same goal. Diagnostic 48 h cases do not play any role in forming the seasonal equation. Seasonal geometry cases define the shape of the reference response and conductivity cases show how it is distorted by the material properties.

Table 1. Numerical case groups.

Case group	Content	Cases	Use in the analysis
48 h diagnostic group	Reference and perturbed cases with changes in initialization, boundary condition, and wall conductivity	17	Ranks the strongest short-term thermal drivers.
Seasonal geometry group	Deep-wall peak responses over excavation ratio, wall depth, and wall thickness	15	Defines the geometric part of the peak-response relation.
Conductivity group	Representative geometries with $k = 1, 2$, and $3\ \mathrm{W\,m^{-1}\,K^{-1}}$	18	Estimates the soil- and wall-conductivity terms.

Figure 1 provides a concise visualization of the numerical basis. The distribution was done on purpose in such way as to have sufficient number of cases for interpreting the data: short-duration cases are numerous enough for ranking of perturbed conditions, geometry cases are sufficient for low-order geometric structure and conductivity cases provide slopes for the investigated range of materials.

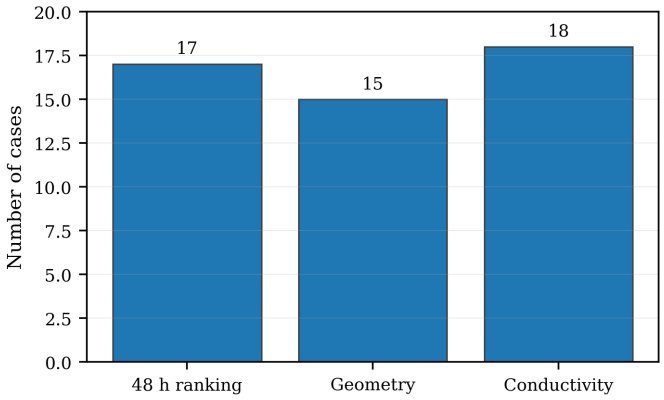

Figure 1. Distribution of numerical cases.

Figure 2 shows that parameter space of the design set is restricted to those variables that enter the surrogate. It should be noted that the plotted points indicate that conductivity cases were chosen not to fill the geometric grid but just at representative locations where material response can be compared without changing the geometrical interpretation.

2.2. Diagnosis measure for short duration

The short-duration class is evaluated based on deviations from the reference value of 48 h,

$$\Delta q_{L,48}^{(i)} = q_{L,48}^{(i)} - q_{L,48}^{\mathrm{ref}}, \qquad q_{L,48}^{\mathrm{ref}} = 33.04\ \mathrm{W/m}. \tag{1}$$

Eq. (1) scales all 48 hour perturbations onto a uniform scale. If the value is positive, then the perturbation has increased the lineal heat exchange compared to the reference, and conversely, if the value is negative, then the perturbation has reduced the lineal heat exchange.

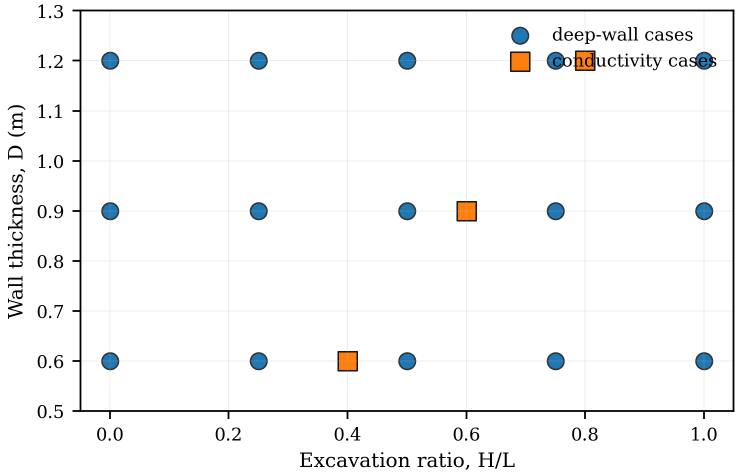

Figure 2. Parameter coverage in the design set.

2.3. Geometry-response relation

The reference-conductivity response of the seasonal geometry category is described by

$$q = q_0 + \Delta q_D \left(\frac{H}{L}\right), \tag{2}$$

where

$$q_0 = 14\,\mathrm{W/m^2}, \qquad \Delta q_D = \frac{6.3}{D} - 5.25. \tag{3}$$

Excavation ratio is used as the exposure parameter in Eq. (2), and Eq. (3) implies that the sensitivity of the response to variation in the exposure factor is dependent on the wall thickness parameter. This interpretation is straightforward: for smaller values of D, the exposed boundary region is still thermally connected to the buried pipe region and becomes more sensitive to increases in H/L. For larger values of D, the pathway length is increased, so the sensitivity decreases.

2.4. Closed-form surrogate

The closed-form surrogate model for peak heat-exchange density is given by

$$q_{\mathrm{peak}} = \beta_0 + \beta_1 \frac{H}{L} + \beta_2 \frac{H}{LD} + \beta_3 (k_s - 2) + \beta_4 (k_c - 2) + \beta_5 \frac{(k_c - 2)}{D}. \tag{4}$$

There is a physical interpretation for each of the terms on the right-hand side of Eq. (4). The unmodified ratio L/H allows the height factor to play a role, the modified term $H/(LD)$ incorporates the stronger influence of the height for thinner walls, the soil conductivity term handles replenishment via the soil, and the two terms involving wall conductivity model the conductive component via the concrete. The conductivity variables are centered around $2\,\mathrm{W\,m^{-1}\,K^{-1}}$ so that the constant remains associated with the reference state.

The values of the coefficients are

$$\beta_0 = 13.936, \quad \beta_1 = -4.763, \quad \beta_2 = 5.883, \quad \beta_3 = 1.233, \quad \beta_4 = 3.314, \quad \beta_5 = 2.314. \tag{5}$$

Substituting Eq. (5) into Eq. (4) gives

$$q_{\mathrm{peak}} = 13.936 + \left(\frac{5.883}{D} - 4.763\right)\frac{H}{L} + 1.233(k_s - 2) + \left(3.314 + \frac{2.314}{D}\right)(k_c - 2). \tag{6}$$

Eq. (6) is the product of the design study at the stage of formulation. From it, it is clear that excavation ratio cannot be considered independently, since its effect is multiplied by $1/D$. Moreover, it is clear why wall conductivity is expected to be a stronger factor than soil conductivity in the given range: the coefficient multiplying $(k_c - 2)$ is orders of magnitude higher than the coefficient multiplying $(k_s - 2)$, moreover, it gets even higher as the wall is getting thinner.

Adequacy of the model was assessed by in-sample fit and leave-one-geometry-out cross-validation. This technique leaves out all geometries of one family and fits the equation on other geometries. In other words, this technique tests whether the chosen equation reflects the geometry-conductivity structure transferable between geometries rather than just matching some isolated data points.

3. Results and discussion

3.1. Short duration ranking

Table 2 shows deviations calculated using Eq. (1). The greatest positive deviations arise when the initial temperature near the wall is lower and when wall conductivity is increased. Deviations due to changes made at the internal or surface boundaries are relatively small.

Table 2. 48 h deviations from the reference case.

Perturbation	**Case**	$\Delta q_{L,48}$ **(W/m)**
Warmer internal boundary only	R01	-0.73
Cooler internal boundary only	R02	$+1.15$
Warmer internal and surface boundaries	R03	-0.84
Cooler internal and surface boundaries	R04	$+1.44$
Cooler upper-wall initial temperature	R05	$+8.02$
Cooler initial ground temperature	R06	$+7.21$
Higher wall thermal conductivity	R07	$+6.04$
Cooler upper wall with higher wall conductivity	R08	$+15.95$
Cooler ground, cooler upper wall, and higher wall conductivity	R09	$+24.49$

The table addresses the short-term aspect of the research question through demonstrating that early heat exchange is controlled by the effects of local heat storage and material properties of walls. The small values in R01–R04 suggest that the moderate variations in boundary conditions outside the pipe zone are less important within the first 48 h, while R05–R09 demonstrate that the initial state of the wall/soil system and k_c affect the heat transfer path directly.

Figure 3 provides a visual representation of the ranking described above. The combined effect of perturbations R09 is much larger than the effects of individual boundary condition changes. Thus, uncertainties in the near-wall heat initialization and the value of concrete thermal conductivity must be addressed preferentially when interpreting short experimental data or simulations.

3.2. Geometry control of seasonal peak exchange

The seasonal geometry effect results from the complex interplay between the excavation ratio and the wall thickness. Figure 4 illustrates the reference curve, which can be derived from Eq. (2) and Eq. (3). For the thin wall, the curve grows sharply with the increasing H/L. In case of thick wall, the curve is almost horizontal. It follows that the increased height of excavation area is thermally meaningful only if the wall allows the effective conductive heat exchange between pipe zone and excavation area.

In other words, excavation ratio is not a general performance parameter in this case. At $D = 0.6$ m, increase in H/L manifests a clear thermal impact; at $D = 1.2$ m, the reaction becomes substantially weaker. The combination of parameters $H/(LD)$ can thus provide more information than the single H/L.

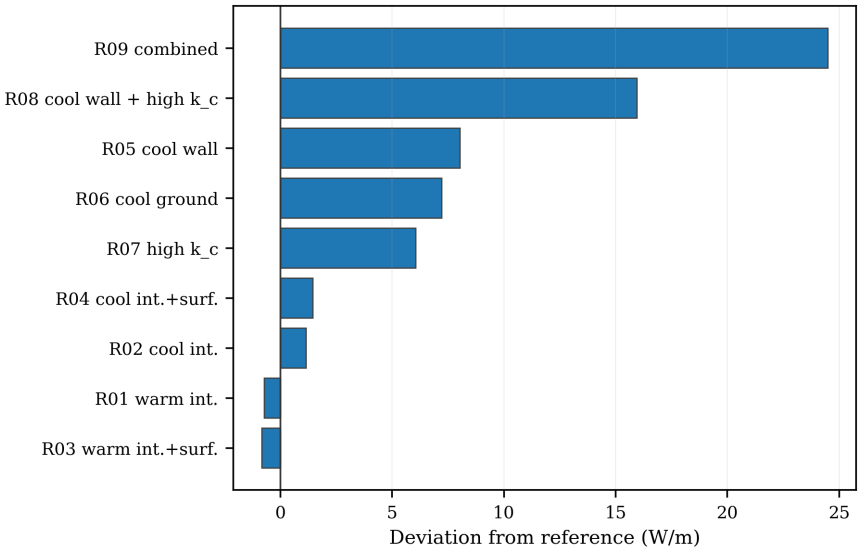

Figure 3. Short-duration heat-exchange deviations.

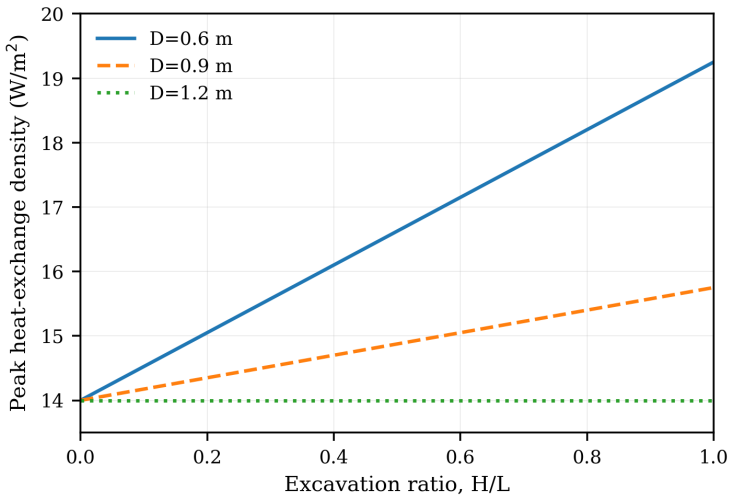

Figure 4. Geometry response at reference conductivity.

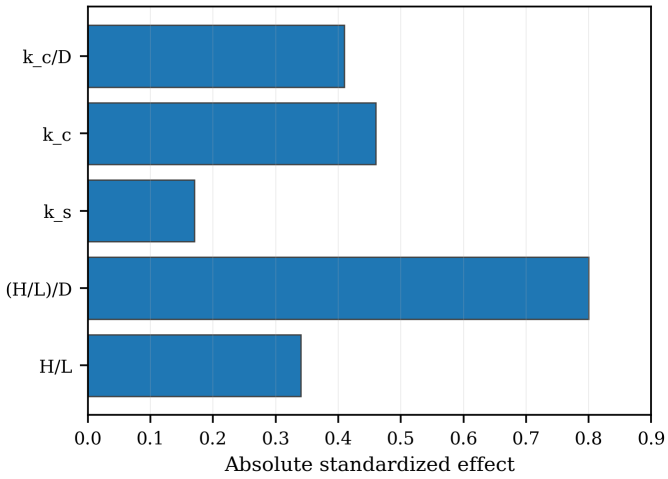

Figure 5. Relative effects in the fitted relation.

It can be seen that Figure 5 corroborates the same observation from the fitted relation. As far as the size of the relative effects, the largest one is attributed to $H/(LD)$, and the pure excavation ratio coefficient appears smaller in its value. The observed pattern is not an artifact of statistics, but is driven by thermal resistance provided by wall thickness. It can be noticed from Figure 5 that wall-conductivity parameters are similar in size to (and sometimes even larger than) the rest of the geometric and soil-conductivity parameters.

3.3. Conductivity effects

There is a significant difference in terms of the influence of the wall and the soil materials within the conductivity group. On average, the first order derivative of soil conductivity is around 1.23 $\mathrm{W\,m^{-2}/W\,m^{-1}\,K^{-1}}$, whereas the first order derivative of wall conductivity is about 6.10 $\mathrm{W\,m^{-2}/W\,m^{-1}\,K^{-1}}$. In other words, wall conductivity is nearly five times more important than soil conductivity in this particular range of parameters.

Asymmetry is clearly seen on Figure 6. This conclusion does not mean that soil parameters are irrelevant. It suggests that concrete itself becomes the dominating resistance in the wall. When performing preliminary design, this result implies the need for specifying the thermal conductivity of concrete precisely and avoiding wall as an insignificant parameter.

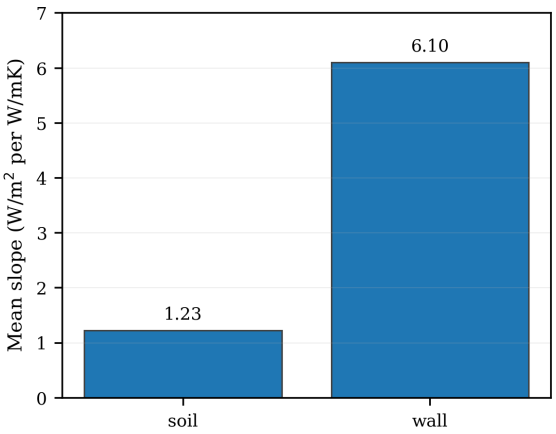

Figure 6. First-order conductivity slopes.

From Figure 7 it follows why the wall-conductivity term is most significant for thin walls. The reason is that the factor that multiplies $(k_c - 2)$ decreases with the increase of D as the excavated-side interface becomes thermally more distant from the pipe region. Therefore, increasing k_c becomes important only if the wall is sufficiently thin.

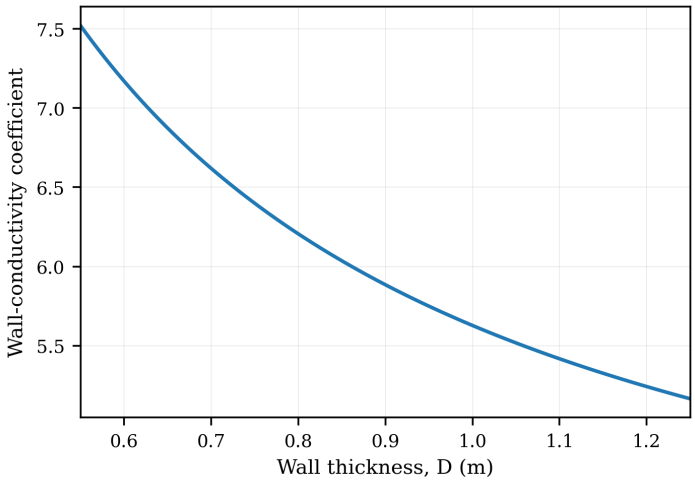

Figure 7. Dependence of the wall-conductivity term on thickness.

3.4. Analytical sensitivity and marginal design gains

The fitted equation can be differentiated to obtain local design sensitivities. Let $x = H/L$. For the compact response

$$q_{\text{peak}} = 13.936 + \left(\frac{5.883}{D} - 4.763\right)x + 1.233(k_s - 2) + \left(3.314 + \frac{2.314}{D}\right)(k_c - 2), \quad (7)$$

the first-order sensitivity vector is

$$\begin{aligned} S_x &= \frac{\partial q}{\partial x} = \frac{5.883}{D} - 4.763, & S_D &= \frac{\partial q}{\partial D} = -\frac{5.883x + 2.314(k_c - 2)}{D^2}, \\ S_s &= \frac{\partial q}{\partial k_s} = 1.233, & S_c &= \frac{\partial q}{\partial k_c} = 3.314 + \frac{2.314}{D}. \end{aligned} \quad (8)$$

The Eq. (8) provides an additional mathematical interpretation which is not possible based on the fit parameters. The rate of change with respect to the excavation ratio depends solely on D, but the rate of change with respect to thickness depends on both x and k_c. In other words, thickness is not just a geometric coordinate, but also the factor which controls the magnitude of the excavation effect and changes its benefits.

Table 3 reveals consistency between the mathematical derivatives and the physical explanation of the response surfaces. For $D = 0.6$ m, an increment of one unit in excavation ratio will produce a significant effect while an increment of one unit in thickness will generate a considerable negative effect. For $D = 1.2$ m, the derivative with respect to excavation ratio is practically zero which indicates that any extra height above the ground has no value since the wall is thick enough to block the boundary effect. The wall conductivity elastic modulus E_{k_c} is high in all three thickness cases, meaning that the percentage change of k_c leads to a significant percentage effect despite decreasing geometric effect.

Table 3. Local sensitivities at $H/L = 0.6$ and $k_s = k_c = 2\ \text{W m}^{-1}\ \text{K}^{-1}$.

D (m)	q	S_x	S_D	S_c	E_{k_c}
0.6	16.96	5.04	−9.81	7.17	0.85
0.9	15.00	1.77	−4.36	5.88	0.78
1.2	14.02	0.14	−2.45	5.24	0.75

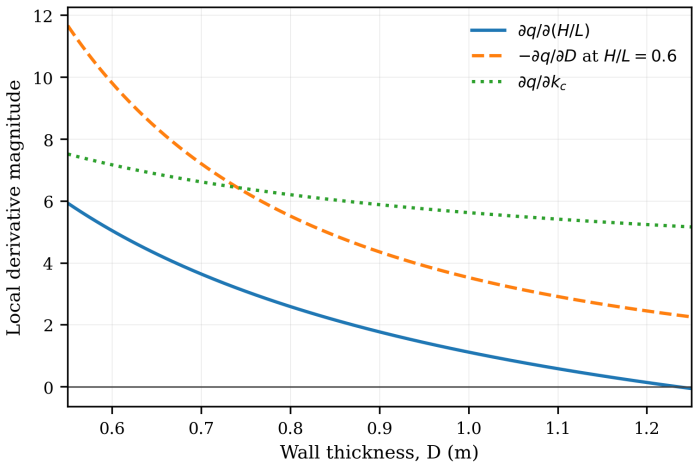

Figure 8. Local sensitivity derivatives.

Figure 8 illustrates the structure of the derivatives over the thickness interval. While the slope with respect to H/L reduces fast with increasing D, the derivative of wall conductivity keeps a high value along the whole range. This analysis clarifies the shape of

the response maps by steepness in thin-wall zones and also proves concrete conductivity as a crucial design parameter despite weak geometric effect.

Finally, the derivative $\partial q/\partial(H/L)$ provides a critical thickness for effective excavation ratio increment:

$$\frac{\partial q}{\partial(H/L)} > 0 \quad \Longrightarrow \quad D < D_{\text{lim}} = \frac{5.883}{4.763} = 1.235 \text{ m}. \tag{9}$$

This Eq. (9) is a purely mathematical justification for the flattening out of the curves with thick walls. Within the existing range of designs, walls up to about 1.2 m have already approached the point when there would be no further useful contribution to the exchange from increased wall exposure. This does not imply that thick walls do not play any heat transfer role but only that their optimization should be achieved by means other than the exposure ratio.

The value of a finite design change may be expressed by the increment

$$\begin{aligned} \Delta q &\approx S_x \Delta x + S_D \Delta D + 1.233 \Delta k_s + S_c \Delta k_c, \\ S_x &= \frac{5.883}{D} - 4.763, \qquad S_c = 3.314 + \frac{2.314}{D}, \\ S_D &= -\frac{5.883x + 2.314(k_c - 2)}{D^2}. \end{aligned} \tag{10}$$

In the case of the representative state $x = 0.6$, $D = 0.9$ m, and $k_s = k_c = 2\ \text{W m}^{-1}\,\text{K}^{-1}$, from Eq. (10) it follows that $S_x = 1.77$, $S_D = -4.36$, and $S_c = 5.88$. Consequently, a decrease in the wall thickness by 0.10 m results in an increase in the peak exchange by about $0.44\ \text{W/m}^2$, whereas an increase in the wall conductivity by only $0.10\ \text{W m}^{-1}\,\text{K}^{-1}$ leads to an increase of about $0.59\ \text{W/m}^2$. These estimates provide numerical support to the previously stated qualitative claim that, within the considered range, even small changes in the wall conductivity are comparable to the possible modifications of geometry.

3.5. Uncertainty propagation in the surrogate response

Since the proposed relation is designed for preliminary design calculations, it is helpful to obtain an assessment of uncertainty propagation from the input variables to the predicted heat exchange. For independent uncertainties in the input variables, one obtains the following first-order propagation formula:

$$\sigma_q^2 \approx (S_x \sigma_x)^2 + (S_D \sigma_D)^2 + (1.233 \sigma_{k_s})^2 + (S_c \sigma_{k_c})^2, \tag{11}$$

where σ_x, σ_D, σ_{k_s}, and σ_{k_c} stand for the standard uncertainties of excavation ratio, thickness, soil conductivity, and wall conductivity, respectively. However, Eq. (11) does not replace a probabilistic simulation; rather, it provides an open and clear mathematical criterion to identify which measurements need to be scrutinized when using the surrogate as a design tool.

For example, when choosing $x = 0.6$, $D = 0.9$ m, $\sigma_x = 0.05$, $\sigma_D = 0.05$ m, and $\sigma_{k_s} = \sigma_{k_c} = 0.20\ \text{W m}^{-1}\,\text{K}^{-1}$, Eq. (11) yields $\sigma_q \approx 1.23\ \text{W/m}^2$. As seen, the bulk of this uncertainty is due to k_c, not the geometrical factors. Thus, the above calculation confirms the engineering recommendation about careful control of concrete thermal conductivity prior to using the surrogate in design.

As seen in Figure 9, the variance contribution for the above representative uncertainty case clearly demonstrates the dominant role of k_c in the uncertainty propagation equation. It is important to note that the dominance of k_c follows from the high value of the wall-conductivity gradient in Eq. (8). In practice, this implies that an accurate geometrical drawing is not sufficient to substitute a poor material input; the latter needs to be controlled if one wants to make conclusions regarding heat exchange differences of a few watts per square meter.

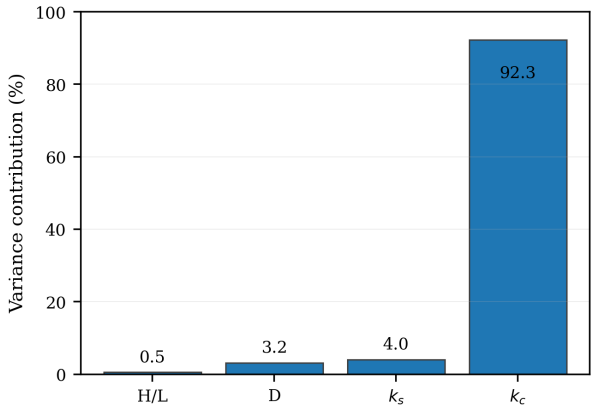

Figure 9. Input uncertainty contributions.

3.6. Accuracy of the surrogate and interpretation of coefficients

The model fits the seasonal case set with an $R^2 = 0.997$ and RMSE of 0.17 W/m^2. Validation using leave-one-geometry-out validation results in $R^2 = 0.985$ and RMSE = 0.37 W/m^2. These numbers suggest that the low order relationship is more than a descriptive formula for the fitted cases, since it preserves some predictive structure even when the geometry families are removed.

Table 4 provides the main engineering interpretation of the equation. It is important to note that the negative sign of the H/L term does not imply any adverse effect of exposure. The term cooperates with the positive $H/(LD)$ so that the value of the exposure is high only when the wall is thermally thin. Likewise, the two wall conductivity terms correspond to both general material improvement and thickness-related thermal resistance reduction.

Table 4. Surrogate coefficients and fit statistics.

Quantity	Value	Interpretation
β_0	13.936	Reference peak heat-exchange density near $k_s = k_c = 2\,\mathrm{W\,m^{-1}\,K^{-1}}$.
$\beta_1(H/L)$	−4.763	Direct excavation-ratio correction.
$\beta_2 H/(LD)$	+5.883	Dominant geometric interaction between exposure and thickness.
$\beta_3(k_s - 2)$	+1.233	Soil-conductivity contribution.
$\beta_4(k_c - 2)$	+3.314	Thickness-independent wall-conductivity contribution.
$\beta_5(k_c - 2)/D$	+2.314	Additional wall-conductivity benefit in thinner walls.
In-sample R^2	0.997	Agreement with the fitted seasonal cases.
Leave-one-geometry-out R^2	0.985	Robustness when geometry families are withheld.
In-sample RMSE	0.17 W/m^2	Average calibration error.
Leave-one-geometry-out RMSE	0.37 W/m^2	Average validation error.

As shown in Figure 10, the fitted values do not deviate from the numerical values much in the whole range of responses. This figure is essential because it ensures the model correctness at the level of heat exchange density prediction, which goes beyond mere coefficients check. The absence of the deviation suggests the possibility of using the surrogate model for early analysis within the analysed range.

3.7. Design reading from the response surfaces

Figure 11 presents the final equation in the form of a response surface under the condition $k_s = k_c = 2\,\mathrm{W\,m^{-1}\,K^{-1}}$. As seen, the contour map is the sharpest in the case of

small D and high H/L, which means the optimal conditions for exploitation of excavation exposure.

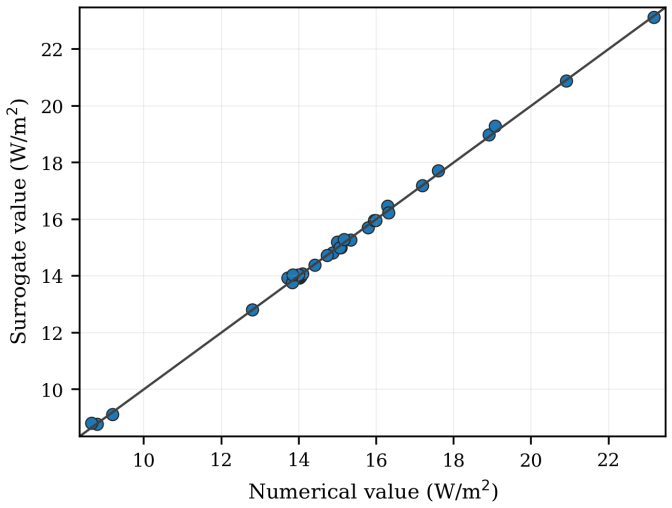

Figure 10. Numerical-surrogate agreement.

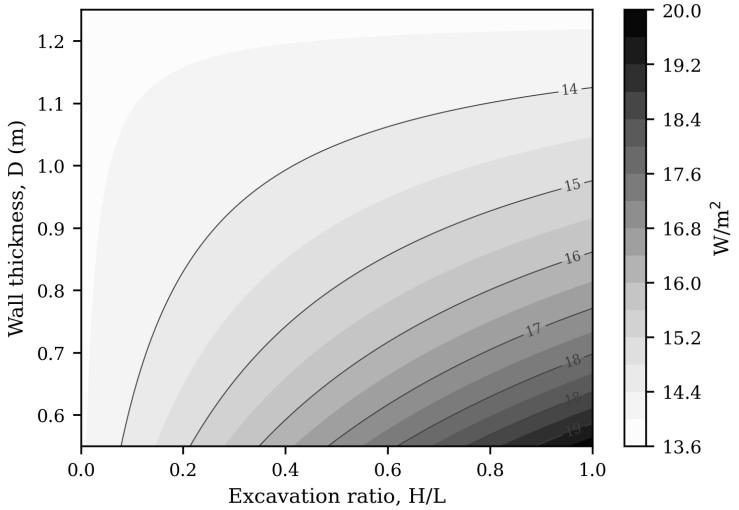

Figure 11. Reference response surface.

The design implication drawn from Figure 11 is clear: for thick walls, an increase in excavation ratio may fail to result in significant thermal performance improvements. In contrast, for thin walls, the same ratio may take the design into the next level of heat exchange. The use of this map as a screening tool for the deep walls is appropriate; shallow walls close to $L = 10$ m represent the limit of applicability due to the influence of proximity to upper boundary on thermal regime.

As can be seen from Figure 12, the increase in k_c moves the curve significantly more upwards compared to that in k_s. This is in line with the structure of coefficients of Eq. (6). In addition, the difference between the curves proves that good geometry is not sufficient to improve the poor conductivity of the wall.

The second reading of design is shown in Figure 13 in terms of wall conductivity versus thickness. The peak response happens at high k_c and low D. This behavior matches the physical meaning of conducting enhancement working along a short thermal path. For initial design purposes, the figure can be used for comparison between material enhancement and thickness in a combined way.

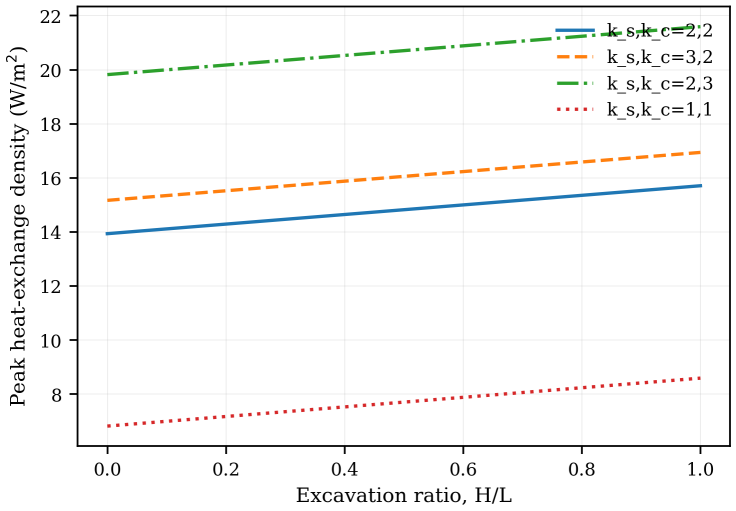

Figure 12. Curves for conductivity states.

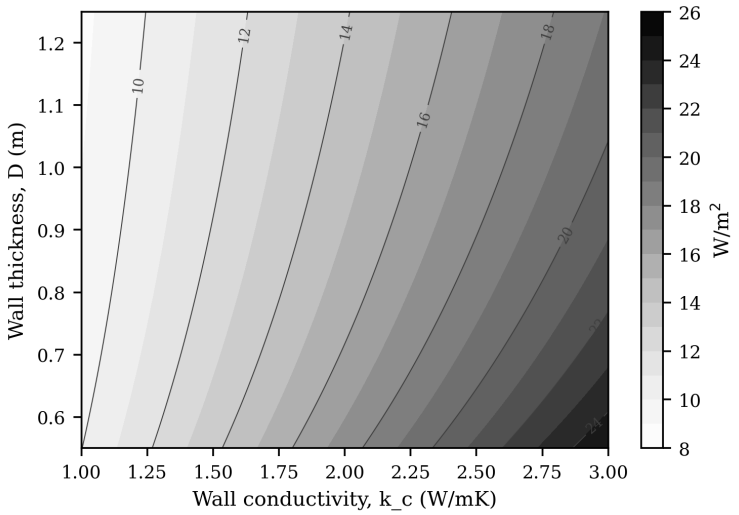

Figure 13. Wall-conductivity response surface.

3.8. Scope and engineering use

The model should be applied within the range of the presented numerical examples. It may be used as a quick tool to compare alternative designs of deep planar retaining walls, perform sensitivity studies, and identify potential thermally advantageous solutions. However, it cannot be used as the only basis for design when the influence of other factors such as groundwater flow, pipe spacing, loading cycles of buildings, construction schedule, or serviceability issues is expected to govern the coupled behavior. Such an analysis needs to be done on a case-by-case basis [19].

Therefore, the surrogate is valuable due to its interpretability. It tells us which variables are important and why. Short-duration heat exchange is governed mostly by the near-wall thermal regime and wall conductivity. Seasonal peak response is governed by the interplay between exposure of excavation and wall thickness. Material improvement works best when it lowers the local wall resistance especially for thin walls. These conclusions are drawn immediately from the relation and the one-panel graphs.

4. Conclusions

This study determined whether the heat exchange at peak heating season in thermally activated planar retaining walls can be represented through a transparent, low-order

surrogate preserving the major geometric and material influences. It was found that the answer is positive in the considered deep wall range. The fitted formula correctly captures the seasonal case set with $R^2 = 0.997$, and retains its good leave-one-geometry-out generalization power with $R^2 = 0.985$, while still being physically meaningful in all terms.

The short-duration analysis revealed that the early heat exchange process depends primarily on the thermal status near the wall and wall conductivity. The boundary condition changes that have a relatively weak effect on the local pipe-wall thermal environment generate relatively small deviations, while the combined influence of wall, ground and k_c initialization changes causes the highest response. It means that the latter three factors require special attention during short-term test and simulation-based calibration.

In the case of seasonal design problem, the major geometric parameter is $H/(LD)$ rather than H/L. The exposure of walls to the excavation is beneficial mostly when the wall is thermally thin enough to experience the effect of the excavated side on the pipe region. The analysis of conductivity effects revealed that the wall conductivity is nearly five times more important than soil conductivity in the considered range, and the relative benefit of increasing k_c rises as D falls.

Practically, the obtained formula gives an explicit screening model for initial assessing geothermal heat exchange of retaining walls, improved through derivative-based sensitivity, local elasticities, interpretation in terms of critical thicknesses, and first order uncertainty propagation. These enhancements allow not only to determine which design variables enhance heat exchange but also reveal the rates of changes of response and dominating sources of uncertainties in predictions. With the help of the presented model, engineers can compare different wall thicknesses, excavation ratios and material conductivities before moving to detailed modeling. However, its major drawback is intended: transparency of design interpretation takes precedence over generality of the equation. Future works should expand the relation by including groundwater flow, pipe layout variables, transient schedules of operation, and field/full scale numerical validation. Within its stated range, the presented equation gives an analytic criterion of selecting walls with high heat exchange potential.

References

[1] Brandl, H. (2006). Energy foundations and other thermo-active ground structures. Géotechnique, 56(2), 81-122.

[2] De Moel, M., Bach, P. M., Bouazza, A., Singh, R. M., & Sun, J. O. (2010). Technological advances and applications of geothermal energy pile foundations and their feasibility in Australia. Renewable and Sustainable Energy Reviews, 14(9), 2683-2696.

[3] McCartney, J. S., Sánchez, M., & Tomac, I. (2016). Energy geotechnics: Advances in subsurface energy recovery, storage, exchange, and waste management. Computers and Geotechnics, 75, 244-256.

[4] Amis, T., Robinson, C. A. W., & Wong, S. (2010). Integrating geothermal loops into the diaphragm walls of the Knightsbridge Palace Hotel project. EMAP-Basements and Underground Structures.

[5] Xia, C., Sun, M., Zhang, G., Xiao, S., & Zou, Y. (2012). Experimental study on geothermal heat exchangers buried in diaphragm walls. Energy and Buildings, 52, 50-55.

[6] Di Donna, A., Cecinato, F., Loveridge, F., & Barla, M. (2017). Energy performance of diaphragm walls used as heat exchangers. Proceedings of the Institution of Civil Engineers-Geotechnical Engineering, 170(3), 232-245.

[7] Bourne-Webb, P. J., Freitas, T. B., & da Costa Gonçalves, R. A. (2016). Thermal and mechanical aspects of the response of embedded retaining walls used as shallow geothermal heat exchangers. Energy and Buildings, 125, 130-141.

[8] Sterpi, D., Coletto, A., & Mauri, L. (2017). Investigation on the behaviour of a thermo-active diaphragm wall by thermo-mechanical analyses. Geomechanics for Energy and the Environment, 9, 1-20.

[9] Dong, S., Li, X., Tang, A. M., Pereira, J. M., Nguyen, V. T., Che, P., & Xiong, Z. (2019). Thermo-mechanical behavior of energy diaphragm wall: Physical and numerical modelling. Applied Thermal Engineering, 146, 243-251.

[10] Rammal, D., Mroueh, H., & Burlon, S. (2020). Thermal behaviour of geothermal diaphragm walls: Evaluation of exchanged thermal power. Renewable energy, 147, 2643-2653.

[11] Makasis, N., & Narsilio, G. A. (2020). Energy diaphragm wall thermal design: The effects of pipe configuration and spacing. Renewable Energy, 154, 476-487.

[12] Di Donna, A., Loveridge, F., Piemontese, M., & Barla, M. (2021). The role of ground conditions on the heat exchange potential of energy walls. Geomechanics for Energy and the Environment, 25, 100199.

[13] Sailer, E., Taborda, D. M., Zdravković, L., & Potts, D. M. (2019). Fundamentals of the coupled thermo-hydro-mechanical behaviour of thermo-active retaining walls. Computers and Geotechnics, 109, 189-203.

[14] Zeng, C., Tang, F., Yuan, Y., Cao, X., Haghighat, F., & Panchabikesan, K. (2021). Thermal performance of energy diaphragm wall (EDW) adjacent to air-conditioned space from the underground-engineering perspective. Geothermics, 91, 102044.
[15] Shafagh, I., Rees, S., Urra Mardaras, I., Curto Jano, M., & Polo Carbayo, M. (2020). A model of a diaphragm wall ground heat exchanger. Energies, 13(2), 300.
[16] Box, G. E., & Draper, N. R. (1987). Empirical model-building and response surfaces. John Wiley & Sons.
[17] Forrester, A., Sobester, A., & Keane, A. (2008). Engineering design via surrogate modelling: a practical guide. John Wiley & Sons.
[18] Myers, R. H., Montgomery, D. C., & Anderson-Cook, C. M. (2016). Response surface methodology: process and product optimization using designed experiments. John Wiley & Sons.
[19] Sterpi, D., Tomaselli, G., & Angelotti, A. (2020). Energy performance of ground heat exchangers embedded in diaphragm walls: Field observations and optimization by numerical modelling. Renewable Energy, 147, 2748-2760.